Electron-Transfer Oxidation of Coenzyme B_{12} Model Compounds and Facile Cleavage of the Cobalt(IV)−Carbon Bond via Charge-Transfer Complexes with Bases. A Negative Temperature Dependence of the Rates

Kei Ohkubo and Shunichi Fukuzumi*

Department of Material and Life Science, Graduate School of Engineering, Osaka University, SORST, Japan Science and Technology Agency, Suita, Osaka 565-0871, Japan

Received: October 14, 2004; In Final Form: November 19, 2004

The electron-transfer oxidation and subsequent cobalt−carbon bond cleavage of vitamin B_{12} model complexes were investigated using cobaloximes, $(DH)_2Co^{III}(R)(L)$, where DH^- = the anion of dimethylglyoxime, R = Me, Et, Ph, $PhCH_2$, and $PhCH(CH_3)$, and L = a substituted pyridine, as coenzyme B_{12} model complexes and $[Fe(bpy)_3](PF_6)_3$ or $[Ru(bpy)_3](PF_6)_3$ (bpy = 2,2′-bipyridine) as a one-electron oxidant. The rapid one-electron oxidation of $(DH)_2Co^{III}(Me)(py)$ (py = pyridine) with the oxidant gives the corresponding Co(IV) complexes, $[(DH)_2Co^{IV}(Me)(py)]^+$, which were well identified by the ESR spectra. The reorganization energy (λ) for the electron-transfer oxidation of $(DH)_2Co(Me)(py)$ was determined from the ESR line broadening of $[(DH)_2Co(Me)(py)]^+$ caused by the electron exchange with $(DH)_2Co(Me)(py)$. The λ value is applied to evaluate the rate constants of photoinduced electron transfer from $(DH)_2Co(Me)(py)$ to photosensitizers in light of the Marcus theory of electron transfer. The Co(IV)−C bond cleavage of $[(DH)_2Co(Me)(py)]^+$ is accelerated significantly by the reaction with a base. The overall activation energy for the second-order rate constants of Co(IV)−C bond cleavage of $[(DH)_2Co^{IV}(Me)(py)]^+$ in the presence of a base is decreased by charge-transfer complex formation with a base, which leads to a negative activation energy for the Co(IV)−C cleavage when either 2-methoxypyridine or 2,6-dimethoxypyridine is used as the base.

Introduction

Coenzyme B_{12} (5′-deoxyadenosylcobalamin, AdoCbl)-dependent rearrangements are initiated by the cobalt−carbon bond dissociation to generate 5′-deoxyadenosyl radical.[1,2] The Co(III)−C bond dissociation energies of various B_{12} model complexes have been determined by Halpern et al. in relation to the bond dissociation mechanisms of coenzyme B_{12}-dependent rearrangement.[3−6] The nonenzymatic thermal bond cleavage of AdoCbl has also been extensively studied by Finke et al., and the activation parameters ($\Delta H^{\ddagger}$ and $\Delta S^{\ddagger}$) of the Co(III)−C bond dissociation have been reported as 33 ± 2 kcal mol^{-1} and 11 ± 2 cal mol^{-1} K^{-1}, respectively.[7,8] Under enzymatic reaction conditions, however, the enzyme enhances the rate of Co−C bond cleavage by a factor up to $10^{12\pm1}$ as compared to that of the free coenzyme.[3−10]

There have been many mechanisms for the origin of the enormous enhancement for the Co−C bond cleavage proposed so far.[11−16] Enzymatic compression of the axial Co−N bond has been proposed to cause transmission of steric compression to the Co−C bond which is activated by the "butterfly"-type upward deformation of the corrin-ring plane.[13,14] Such deformation may be made possible by the flexibility of the corrin ring, which has been shown to be in sharp contrast with the rigidity of the porphyrin ring.[5] However, the X-ray crystal structure of coenzyme B_{12}-dependent methylmalonyl-CoA (MMCoA) mutase has revealed that B_{12}'s appended 5,6-dimethylbenzimidazole base is not bound directly to cobalt in MMCoA mutase as previously believed, but that a protein side-chain histidine imidazole serves as the axial base coordinated with cobalt.[17] Since then, the actual role of the axial base in both Co−C bond cleavage and heterolysis has been studied extensively.[16,18]

On the other hand, it has been reported that the Co(II)−C bond of methylcobalamin is significantly weakened when compared to the Co(III)−C bond.[19] Although the electron-transfer reduction of AdoCbl is hardly predicted for the mechanism of any adenosylcobalamin-dependent or methylcobalamin-dependent enzymes, the comparison of bond cleavage rates for reduced and unreduced cobamides provided valuable insight into the nature of the Co−C bond.[19] The Co(II)−C bond cleavage rate was too fast to be determined at room temperature; therefore the rate was determined electrochemically at temperatures below −30 °C.[20] The one-electron reduction of methylcobalamin leads to population of the Co−C σ^* orbital, thus facilitating the cleavage.[20]

Alternatively, the one-electron oxidation may lead to depopulation of the Co−C σ orbital, also facilitating the Co−C bond cleavage as indicated by Halpern et al.[21,22] In this context, we have recently reported the one-electron oxidized organocobalt porphyrins $([(TPP)Co(Me)(L)]^+$, TPP^{2-} = the dianion of tetraphenylporphyrin, L = substituted pyridines) have d^5 cobalt(IV) character depending on R or L and that the dissociation energies of the Co(IV)−C bond are significantly smaller than those of the corresponding Co(III)−C bond.[23] We have also reported facile bond cleavage for the Co(IV)−C bond of dialkylcobalt(IV) complexes when compared to the slow cleavage of the corresponding dialkylcobalt(III) complexes, which require thermal or photochemical activation.[24] However, the dynamics of the electron-transfer oxidation and the subsequent Co(IV)−C bond cleavage of B_{12} model complexes have yet to be reported.

We report, herein, the first extensive kinetic data for the electron-transfer oxidation of coenzyme B_{12} model complexes,

10.1021/jp0453008 CCC: $30.25 © 2005 American Chemical Society
Published on Web 01/20/2005

σ-bonded organocobaloximes, $[(DH)_2Co^{IV}(R)(L)]^+$ (DH^- = the anion of dimethylglyoxime, R = Me, Et, Ph, $PhCH_2$, and $PhCH(CH_3)$, and L = substituted pyridines), and the subsequent facile Co(IV)−C bond cleavage in the presence of bases. The reorganization energy for the electron-transfer oxidation of $(DH)_2Co(Me)(py)$ (py = pyridine) was determined from the ESR line broadening of $[(DH)_2Co^{IV}(Me)(py)]^+$ due to the electron self-exchange with $(DH)_2Co^{III}(Me)(py)$. The Co(IV)−C bond cleavage rate of $[(DH)_2Co(Me)(py)]^+$ is accelerated significantly by the reaction with a base, when the charge-transfer complexes are formed between $[(DH)_2Co(Me)(py)]^+$ and bases. The most striking feature of the Co(IV)−C bond cleavage with bases is that the temperature dependence of the second-order rate constants exhibit negative activation enthalpies, e.g., −9.5 kJ mol^{-1} in the Co(IV)−C bond cleavage with 2,6-dimethoxypyrindine. Such negative activation enthalpy has never been observed for any bond cleavage reaction, but has been observed in a number of cases, including Diels−Alder, hydride-transfer, and electron-transfer reactions via charge-transfer complexes, which lie along the reaction pathway.[25−27] Although the Co(IV)−C bond cleavage may not be involved in the facile Co−C bond cleavage in the enzymatic reaction, the observation of a negative temperature dependence on the facile Co(IV)−C bond cleavage provides valuable insight into the cobalt−carbon bond activation mechanism.

Experimental Section

Materials. Cobalt chloride and iron sulfate were purchased from Nacalai Tesque. Dimethylglyoxime and 2,2′-bipyridine were purchased from Wako Pure Chemicals. Organocobaloximes, $(DH)_2Co(R)(L)$ (R = Me, Et, Ph, $PhCH_2$, and $PhCH(CH_3)$, L = substituted pyridines and H_2O) were prepared by following the literature method.[28−31] They are purified by a Soxhlet extraction with dichloromethane, and then recrystallized with dichloromethane/acetone. ^{1}H NMR spectra were measured on a JEOL NMR spectrometer, GSX-400 (400 MHz) and JEOL JMN-AL300 (300 MHz) (see Supporting Information (S1) for the NMR data of $(DH)_2Co(R)(L)$). Since the $(DH)_2Co(R)(L)$ compounds are light sensitive,[29,31] the compounds were kept in the dark and all experiments were carried out in the dark.

Tris(2,2′-bipyridine)iron(III) hexafluorophosphate, $[Fe(bpy)_3](PF_6)_3$, was prepared from a reaction between iron(II)sulfate heptahydrate and 2,2′-bipyridine followed by oxidation of the resulting iron(II) complex by ceric sulfate in aqueous H_2SO_4.[32] Tris(2,2′-bipyridine)ruthenium dichloride hexahydrate, $[Ru(bpy)_3]Cl_2\cdot 6H_2O$, was obtained commercially from Aldrich. The oxidation of $[Ru(bpy)_3]Cl_2$ with lead dioxide in aqueous H_2SO_4 produces $[Ru(bpy)_3]^{3+}$ which was isolated as the PF_6 salt, $[Ru(bpy)_3](PF_6)_3$.[33] Phenanthrene, pyrene, and anthracene used as photosensitizers were obtained commercially. Pyridine and substituted pyridines (3,5-dichloropyridine, 4-cyanopyridine, 3-chloropyridine, 3-picoline, 3,4-lutidine, 4-(dimethylamino)-pyridine, 3-bromopyridine, 2-picoline, 4-picoline, 4-aminopyridine, 3-butylpyridine, 2-methoxypyridine, and 2,6-dimethoxypyridine) were also obtained commercially and purified using standard methods.[34] Tetrabutylammonium perchlorate (TBAP), obtained from Fluka Fine Chemical, was recrystallized from ethanol and dried in vacuo prior to use. Acetonitrile used as a solvent was purified and dried by the standard procedure.[34] Acetonitrile-d_3 (CD_3CN) was obtained from EURI SO-TOP, France.

Reaction Procedure. Typically, $(DH)_2Co(R)(py)$ (R = Me and Et, 1.0×10^{-3} M) and $[Fe(bpy)_3](PF_6)_3$ (2.0×10^{-3} M) were added to an NMR tube which contained deaerated CD_3CN (0.60 cm^3) under 1 atm of argon. The products were identified by comparing the ^{1}H NMR spectra with those of authentic samples. ^{1}H NMR (400 MHz, CD_3CN): *N*-methylpyridinium ion, δ 4.30 (s, 3H), 8.0−9.2 (m, 5H); *N*-ethylpyridinium ion, δ 1.57 (t, 3H, J = 7.3 Hz), 4.54 (q, 2H, J = 7.3 Hz), 7.5−9.0 (m, 5H).

Kinetic Measurements. Kinetic measurements of the oxidation of $(DH)_2Co(R)(L)$ with $[Fe(bpy)_3](PF_6)_3$ in MeCN were performed on a Hewlett-Packard 8453 photodiode array spectrophotometer and a Shimadzu UV-160A spectrophotometer which was thermostated from 298 to 328 K. Typically, a deaerated MeCN solution of $[Fe(bpy)_3](PF_6)_3$ (1.0×10^{-4} M) was added to an MeCN solution of $(DH)_2Co(Me)(py)$ (1.7×10^{-5} M) by means of a microsyringe in a quartz cuvette (i.d. 10 mm) under Ar with stirring. All kinetic measurements were carried out with the concentrations of $[Fe(bpy)_3](PF_6)_3$ maintained at >10-fold excess of the concentrations of $(DH)_2Co(R)(L)$. Rates of the oxidation of $(DH)_2Co(R)(L)$ with $[Fe(bpy)_3](PF_6)_3$ in MeCN were monitored by measuring the increase of absorbance due to $[Fe(bpy)_3]^{2+}$ at λ_{max} = 520 nm ($\epsilon_{max} = 8.7 \times 10^3$ M^{-1} cm^{-1}) in MeCN at 298 K.[35] Kinetic measurements of the oxidation of $(DH)_2Co(Me)(py)$ with $[Fe(bpy)_3](PF_6)_3$ in the presence of pyridine derivatives in MeCN were performed on a UNISOKU RSP-601 stopped-flow rapid scan spectrophotometer with the MOS-type highly sensitive photodiode array at various temperatures (238−298 K) using an UNISOKU thermostated cell holder designed for low-temperature experiments. Typically, MeCN solutions of pyridine derivatives and $[(DH)_2Co^{IV}(Me)(py)]^+$ (2.2×10^{-5} M) produced by mixing $Fe(bpy)^{3+}$ (5.0×10^{-5} M) with $(DH)_2Co^{III}(Me)(py)$ (2.2×10^{-5} M) were transferred into the spectrophotometric cells. The first-order rate constants were determined by least-squares curve fits using a personal computer. The first-order plots were linear for 3 or more half-lives with the correlation coefficient $\rho > 0.999$.

Fluorescence Quenching. Quenching experiments of the fluorescence of phenanthrene, anthracene, pyrene, and $[Ru(bpy)_3]^{2+}$ were performed using a Shimadzu RF 5300PC fluorescence spectrophotometer. The excitation wavelengths were 345, 375, 372, and 450 nm for phenanthrene, anthracene, pyrene, and $[Ru(bpy)_3]^{2+}$ in MeCN, respectively. The monitoring wavelengths were those corresponding to the maxima of the emission bands at λ = 488, 398, 460, and 600 nm, respectively. The solutions were deoxygenated by argon purging for 10 min prior to the measurements. Relative emission intensities were measured for an MeCN solution containing photosensitizer (2.0×10^{-5} M) with $(DH)_2Co(Me)(py)$ at various concentrations (1.5×10^{-5} to 2.5×10^{-4} M). There was no change in the shape but there was a change in the intensity of the fluorescence spectrum from the addition of $(DH)_2Co(Me)(py)$. The Stern−Volmer relationship (eq 1) was obtained for the ratio of the emission intensities in the absence and presence of $(DH)_2Co(Me)(py)$ (I_0/I) and the concentrations of $(DH)_2Co(Me)(py)$.

$$I_0/I = 1 + K_{SV}[(DH)_2Co(Me)(py)] \quad (1)$$

The observed quenching rate constants k_q ($=K_{SV}\tau^{-1}$) were obtained from the Stern−Volmer constants K_{SV} and the emission lifetimes τ.

Cyclic Voltammetry. Cyclic voltammetry measurements were performed at 298 K on a BAS 100W electrochemical analyzer in deaerated MeCN containing 0.1 M NBu_4ClO_4 as the supporting electrolyte. A conventional three-electrode cell was used with a gold working electrode (surface area of 0.3

TABLE 1: One-Electron Oxidation Potentials (E°_{ox} vs SCE) of $(DH)_2Co(Me)(L)$ and ESR Parameters ($g_{||}$ and $A_{||(Co)}$) of $[(DH)_2Co(Me)(L)]^+$ in MeCN

no.	L	pK_a[a]	E°_{ox}[b] (V)	$g_{||}$	$A_{||(Co)}$ (G)
1	3,5-Cl_2py	0.67	0.84	2.0206	26.7
2	4-CNpy	1.86	0.80	2.0215	26.4
3	3-Clpy	2.81	0.84	2.0206	26.3
4	3-Brpy	2.84	0.83	2.0199	26.2
5	py	5.28	0.85	2.0212	26.3
6	3-Mepy	5.79	0.82	2.0213	26.7
7	2-Mepy	5.96	0.81	nd	nd
8	4-Mepy	5.98	0.84	2.0244	26.6
9	3,4-Me_2py	6.46	0.82	2.0211	26.9
10	4-Me_2Npy	9.71	0.80	2.0216	29.1
11	3-Bupy		0.81	nd	nd
12	H_2O	7.00	0.86	2.0254[c]	27.3[c]

[a] Taken from ref 38. [b] Containing 0.1 M TBAP. [c] Determined in MeOH/MeCN (1:1 v/v).

mm^2) and a platinum wire as the counter electrode. The Pt working electrode (BAS) was polished with a BAS polishing alumina suspension and rinsed with acetone before use. The measured potentials were recorded with respect to the Ag/$AgNO_3$ (0.01 M) reference electrode. All potentials (vs Ag/Ag^+) were converted to values vs SCE by adding 0.29 V.[36] The $E_{1/2}$ value of ferrocene used as a standard is 0.37 V vs SCE in MeCN under the present experimental conditions. All electrochemical measurements were carried out under 1 atm of argon.

ESR Measurements. ESR spectra of $[(DH)_2Co(R)(py)]^+$ in MeCN were measured with a JEOL X-band JES-RE1XE spectrometer and were recorded under nonsaturating microwave power conditions. The magnitude of the modulation was chosen to optimize the resolution and the signal to noise ratio (S/N) of the observed spectra. The g values were calibrated using an Mn^{2+} marker, and the hyperfine coupling constants were determined by a computer simulation using a Calleo ESR II program coded by Calleo Scientific Software Publishers.

Theoretical Calculations. Density-functional theory (DFT) calculations were performed on a COMPAQ DS20E computer. The ionization potentials (I_p) of pyridine derivatives were determined from the energy differences between neutral and radical cations.[37] Geometry optimizations of pyridine derivatives and their radical cations were carried out using the B3LYP functional and 6-31G** basis set with the restricted and unrestricted Hartree−Fock formalism as implemented in the Gaussian 98 program.

Results and Discussion

Electron-Transfer Oxidation of $(DH)_2Co^{III}(R)(L)$. The one-electron oxidation potentials (E°_{ox} vs SCE) of $(DH)_2Co^{III}(R)(H_2O)$ in an aqueous solution were reported previously as 0.849 V (R = p-$CH_3C_6H_4CH_2$) and 0.902 V (R = Me).[21] The E°_{ox} values of $(DH)_2Co^{III}(R)(L)$ (R = Me, Et, Ph, $PhCH_2$, and $PhCH(CH_3)$, L = various pyridines and H_2O) in MeCN were also readily determined by the cyclic voltammograms which give the reversible one-electron redox waves (see Supporting Information S2). No second oxidation wave was observed in the potential region less than 1.5 V. The E°_{ox} values of $(DH)_2Co^{III}(Me)(L)$ with different axial base pyridine ligands (L) are listed in Table 1 together with the pK_a values of L.[38] The E°_{ox} values of $(DH)_2Co^{III}(R)(py)$ with different R groups (R = Me, Et, Ph, $PhCH_2$, and $PhCH(CH_3)$, py = pyridine) are also listed in Table 2. The cyclic voltammograms of all $(DH)_2Co(R)(py)$ complexes in Tables 1 and 2 show reversible waves in MeCN even at a slow scan rate (20 mV s^{-1}) at 298 K, indicating that the Co−C bond cleavage in $[(DH)_2Co(R)(L)]^+$ occurs at a much slower rate than the cyclic voltammetry time scale.

TABLE 2: One-Electron Oxidation Potentials (E°_{ox} vs SCE) of $(DH)_2Co(R)(py)$ and ESR Parameters ($g_{||}$ and $A_{||(Co)}$) of $[(DH)_2Co(R)(py)]^+$ in MeCN

R	E°_{ox}[a] (V)	$g_{||}$	$A_{||Co}$ (G)
$PhCH(CH_3)$	0.80	2.0345	26.3
$PhCH_2$	0.80	2.0344	26.4
Et	0.82	2.0319	26.6
Ph	0.86	2.0223	26.2

[a] Containing 0.1 M TBAP.

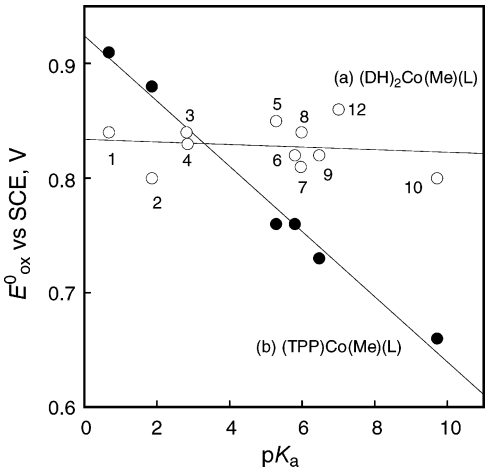

Figure 1. Dependence of the one-electron oxidation potential (E°_{ox}) of (a) $(DH)_2Co(Me)(L)$ (○) and (b) (TPP)Co(Me)(L) (●)[23] on the pK_a of L. Numbers refer to L in Table 1.

The E°_{ox} values of $(DH)_2Co(Me)(L)$ are nearly constant regardless of the pK_a value of L,[38] as shown in Figure 1 (open circles). This is in sharp contrast to those of (TPP)Co(Me)(L) (TPP^{2-} = the dianion of tetraphenylporphyrin, L = substituted pyridines) which decrease with an increase in the pK_a of L (closed circles in Figure 1).[23]

Thisdifference in the dependence of E°_{ox} on pK_a between $(DH)_2Co(Me)(L)$ and (TPP)Co(Me)(L) may result from the difference in the flexibility of $(DH)_2$ and TPP rings. As the pK_a of L increases, the electron density on the metal also increases, leading to the negative shift of the E°_{ox} value in the case of (TPP)-Co(Me)(L) as shown in Figure 1b. In the case of $(DH)_2$Co-(Me)(L), however, the stronger binding of L with the larger pK_a value results in the deformation of the $(DH)_2$ ring, which leads to the weaker binding of Co with nitrogens of $(DH)_2$ rings. These opposite effects cancel each other out to make the E°_{ox} value constant regardless of the pK_a of L as shown in Figure 1.

The one-electron oxidation of $(DH)_2Co^{III}(R)(py)$ has been performed using $[Fe(bpy)_3]^{3+}$ as an oxidant. Since the one-electron reduction potential of $[Fe(bpy)_3]^{3+}$ in MeCN (E°_{red} = 1.04 V vs SCE) is more positive than the one-electron oxidation potentials of $(DH)_2Co^{III}(R)(py)$ (E°_{ox} = 0.85 V vs SCE) but less positive than the second oxidation potentials, only one-electron oxidation of $(DH)_2Co^{III}(R)(py)$ is expected to occur. The one-electron oxidized complexes, $[(DH)_2Co^{IV}(Me)(L)]^+$ with a series of L groups and $[(DH)_2Co^{IV}(R)(py)]^+$ with different R groups, were produced by the one-electron oxidation of $(DH)_2Co(R)$-(L) with $[Fe(bpy)_3]^{3+}$. The ESR spectra were measured in frozen MeCN at 153 K. The ESR spectra revealed the characteristic patterns of eight hyperfine lines from the interaction of the unpaired electron with one cobalt nucleus (I = 7/2, see Supporting Information S3). The ESR parameters ($g_{||}$ and $A_{||(Co)}$) are also listed in Tables 1 and 2. The $g_{||}$ and $A_{||(Co)}$ values of

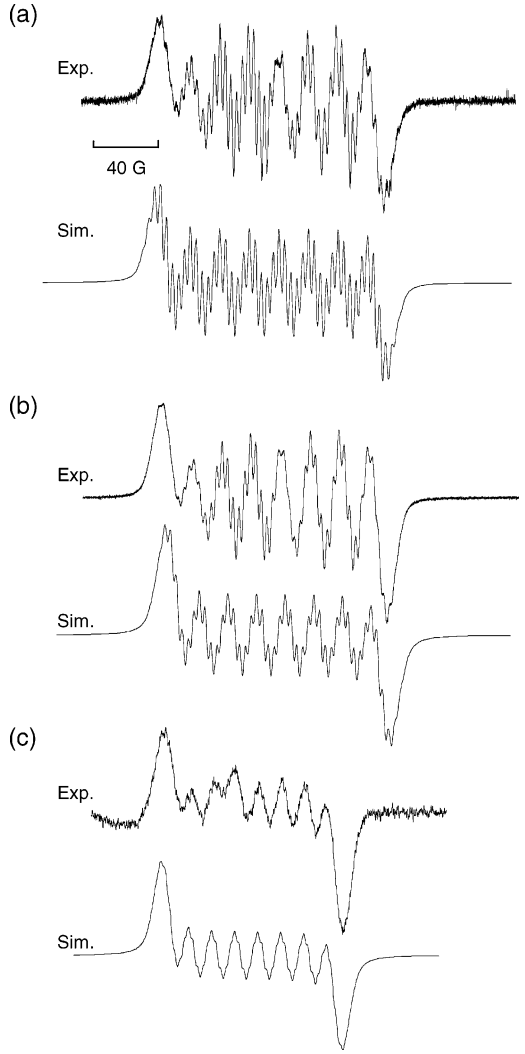

Figure 2. ESR spectra of $[(DH)_2Co^{IV}(Me)(py)]^+$ generated by the electron-transfer oxidation of $(DH)_2Co(Me)(py)$ ((a) 6.0×10^{-3}, (b) 2.0×10^{-2}, and (c) 2.8×10^{-2} M) with $Fe(bpy)_3(PF_6)_3$ (5.0×10^{-4} M) in MeCN at 243 K and computer simulation spectra with $g = 2.0254$, $a(Co) = 13.9$ G, and $a(4N) = 2.5$ G, and ΔH_{msl} = (a) 1.8, (b) 2.4, and (c) 3.0 G.

$[(DH)_2Co(R)(L)]^+$ are insensitive to the type of R and the pK_a of L, and they are virtually the same as those of $[(DH)_2Co(R)(H_2O)]^+$, which have previously been identified as the corresponding organocobalt(IV) species.[23,39−41] Thus, the site of electron removal from all $(DH)_2Co(R)(L)$ complexes is the cobalt atom rather than the $(DH)_2$ ligand.

The ESR spectrum of $[(DH)_2Co(Me)(py)]^+$ produced by the one-electron oxidation of $(DH)_2Co(Me)(py)$ with $[Fe(bpy)_3]^{3+}$ was observed in MeCN at 243 K as shown in Figure 2 which reveals the characteristic patterns of eight hyperfine lines from the interaction of the unpaired electron with one cobalt nucleus ($I = 7/2$) and four equivalent nitrogens of the $(DH)_2$ ligand. The ESR parameters ($g = 2.0254$, $a(Co) = 13.9$ G, and $a(4N) = 2.5$ G) are essentially the same as those reported for $[(DH)_2Co(Me)(H_2O)]^+$.[21,42]

The hyperfine splitting constants and the maximum slope line widths (ΔH_{msl}) were determined from a computer simulation of the ESR spectrum. The ΔH_{msl} value thus determined increases linearly with an increase in the concentration of $(DH)_2Co(Me)(py)$ as shown in Figure 2a−c. The line width variations of the ESR spectra can be used to investigate the rate processes involving the radical species.[42] The rate constants (k_{ex}) of electron self-exchange reactions between $(DH)_2Co(Me)(py)$ and $[(DH)_2Co(Me)(py)]^+$ (eq 2) were determined using eq 3

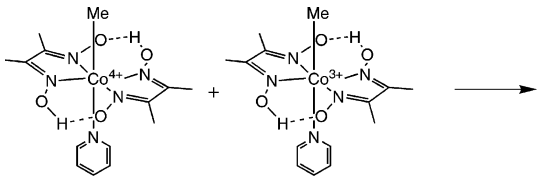

$$[(DH)_2Co^{III}(Me)(py)] + [(DH)_2Co^{IV}(Me)(py)]^+ \quad (2)$$

$$k_{ex} = \frac{1.52 \times 10^7 (\Delta H_{msl} - \Delta H^\circ_{msl})}{(1 - P_i)[(DH)_2Co(Me)(py)]} \quad (3)$$

where ΔH_{msl} and ΔH°_{msl} are the maximum slope line width of the ESR spectra in the presence and absence of $(DH)_2Co^{III}(Me)(py)$, respectively, and P_i is a statistical factor which can be taken as nearly zero.[43] The k_{ex} value determined from the slope of the linear plot of ΔH_{msl} vs $[(DH)_2Co(Me)(py)]$ is 8.4×10^8 M^{-1} s^{-1} (see Supporting Information S4). The reorganization energy (λ) of electron self-exchange between $(DH)_2Co^{III}(Me)(py)$ and $[(DH)_2Co^{IV}(Me)(py)]^+$ is determined from the k_{ex} value as 9.1 kcal mol^{-1} using eq 4

$$\lambda = 4RT \ln[Z\{(k_{ex})^{-1} - (k_{diff})^{-1}\}] \quad (4)$$

where Z is the collision frequency (1×10^{11} M^{-1} s^{-1}) and k_{diff} is the diffusion-limited value in MeCN (2.0×10^{10} M^{-1} s^{-1}).[44] The k_{ex} value of Co(IV)/Co(III) is faster than that of reported Co(II)/Co(III) systems (9.3×10^{-2} to 9.5×10^4 M^{-1} s^{-1}).[45] The λ values are smaller than those of fast electron-transfer exchange systems such as *p*-benzoquinone/semiquinone radical anion (13 kcal mol^{-1} in DMF).[46] The small $a(4N)$ value (2.5 G) of $[(DH)_2Co(Me)(py)]^+$ (cf. $a(4N) = 16$ G for $Cu(DH)_2$) indicates that the unpaired electron is the p-type $d_{x^2-y^2}$ rather than the σ-type d_{xy} metal orbital (the coordinate system adopted for $[(DH)_2Co(Me)(py)]^+$ has the z axis along R−Co−py with the x and y axes in the molecular plane bisecting the N−Co−N angles).[40] Removal of an electron from the $d_{x^2-y^2}$ orbital results in little structural change on the electron-transfer oxidation of $(DH)_2Co(Me)(py)$. This may be the reason for the small λ value of the electron self-exchange between $(DH)_2Co(Me)(py)$ and $[(DH)_2Co(Me)(py)]^+$.

The fluorescence of phenanthrene was quenched by $(DH)_2Co(Me)(py)$ by electron transfer from $(DH)_2Co(Me)(py)$ to the singlet excited state of phenanthrene. The fluorescence of anthracene, pyrene, and $[Ru(bpy)_3]^{2+}$ is also quenched efficiently by $(DH)_2Co(Me)(py)$. The electron-transfer rate constants (k_{et}) of the fluorescence quenching are determined from the slopes of the Stern−Volmer plots and the lifetime of the singlet excited state (see Experimental Section). The free energy change of photoinduced electron transfer from $(DH)_2Co(Me)(py)$ to the singlet excited state (ΔG°_{et} in electronvolts) is given by eq 5

$$\Delta G^\circ_{et} = e(E^\circ_{ox} - E^\circ_{red}) \quad (5)$$

where e is elementary charge, E°_{ox} is the one-electron oxidation potential of $(DH)_2Co(Me)(py)$, and E°_{red} is the one-electron reduction potential of the singlet excited-state electron acceptor.[47,48] The ΔG°_{et} values are largely negative as listed in Table 3, indicating that the fluorescence quenching occurs efficiently via photoinduced electron transfer from $(DH)_2Co(Me)(py)$ to the singlet excited state of the electron acceptor. The rate

TABLE 3: Fluorescence Lifetimes (τ) and Reduction Potentials (E°_{red}) of the Singlet Excited State of Photosensitizers, Free Energy Change of Electron Transfer ($-\Delta G^{\circ}_{et}$), and Rate Constants (k_{et}) of Photoinduced Electron Transfer from $(DH)_2Co(Me)(py)$ to the Singlet Excited State of Photosensitizers in Deaerated MeCN at 298 K

no.	oxidant[a]	τ (ns)[b]	E°_{red} vs SCE (V)	ΔG°_{et} (eV)	k_{et} (M^{-1} s^{-1})
1	phenanthrene*	61	1.39	−0.54	2.0×10^{10}
2	anthracene	5.3	1.38	−0.53	1.9×10^{10}
3	pyrene*	475	1.23	−0.38	1.2×10^{10}
4	$(DH)_2Co(Me)(py)$[c]		0.85	0	1.9×10^{10}[d] (8.4×10^{8})[e]
5	$[Ru(bpy)_3]^{2+}$*	850	0.77	0.08	2.6×10^{8}

[a] Asterisk (*) denotes the excited state. [b] Taken from refs 47 and 48. [c] Electron self-exchange rate constant between $(DH)_2Co^{III}(Me)(py)$ and $[(DH)_2Co^{IV}(Me)(py)]^+$ determined from the line width variation of ESR spectra. [d] Value at 298 K evaluated from the λ value using eq 4. [e] Determined at 243 K.

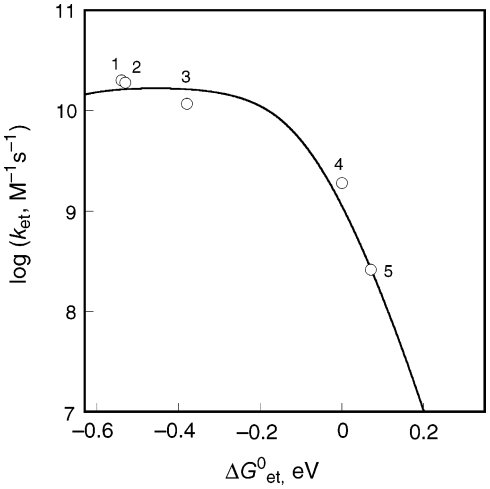

Figure 3. Plot of k_{et} vs the free energy change of electron transfer (ΔG°_{et}) for fluorescence quenching of various photosensitizers by $(DH)_2Co(Me)(py)$ in MeCN at 298 K. The curve represents the best fit to the Marcus equation (eq 6). Numbers refer to photosensitizers in Table 3.

constants (k_{et}) of the fluorescence quenching via photoinduced electron transfer are listed in Table 3, where the k_{et} values are in the range of 1.2×10^{10} to 2.0×10^{10} M^{-1} s^{-1}, being close to the diffusion limit in MeCN at 298 K.[44] A plot of k_{et} vs ΔG°_{et} is shown in Figure 3 which demonstrates a typical dependence of the rate constant for photoinduced electron-transfer reactions on the free energy change of electron transfer (ΔG°_{et}); the log k_{et} value increases with a decrease in ΔG°_{et} to reach a diffusion-limited value ($k_{diff} = 2.0 \times 10^{10}$ M^{-1} s^{-1} in MeCN).[44] The dependence of k_{et} on ΔG°_{et} for adiabatic outer-sphere electron transfer has been well established by Marcus as given by eq 6

$$\frac{1}{k_{et}} = \frac{1}{k_{diff}} + \frac{1}{Z \exp[(-\lambda/4)(1 + \Delta G^{\circ}_{et}/\lambda)^2/k_B T]} \quad (6)$$

where λ is the reorganization energy of electron transfer and k_B is the Boltzmann constant.[44,49] By fitting the data in Figure 3 with the Marcus equation for bimolecular ET reactions (eq 6), we obtained a λ value of 10.5 kcal mol^{-1}, which agrees with the value from the change of the line width of the ESR spectra.

Rates of Co(IV)−C Bond Cleavage. As expected from the small λ value in Figure 4, the first one-electron oxidation of $(DH)_2Co(Me)(py)$ with $[Fe(bpy)_3]^{3+}$ was too fast to be monitored even with a stopped-flow technique. However, the initial fast one-electron oxidation of $(DH)_2Co^{III}(Me)(py)$ with more than 2 equiv of $[Fe(bpy)_3]^{3+}$ is followed by the second one-electron oxidation which is much slower than the first oxidation. A typical example for the spectral change is shown in Figure 4, where the absorption band due to $[Fe(bpy)_3]^{2+}$ appears stepwise in the oxidation of $(DH)_2Co(Me)(py)$ with $[Fe(bpy)_3]^{3+}$. The stoichiometry of the two-electron oxidation of the reaction is given by eq 7 which is based on product analysis (see Experimental Section).

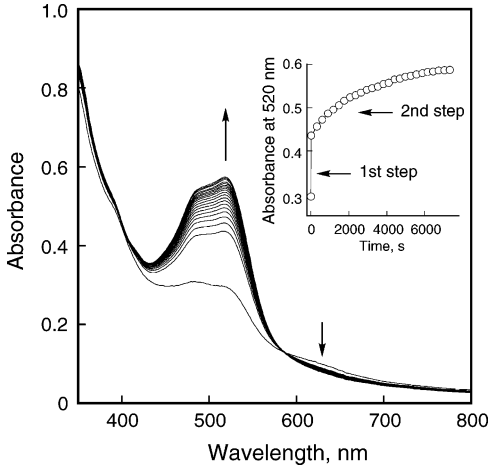

Figure 4. Visible spectral change observed in electron transfer from $(DH)_2Co(Me)(py)$ (1.7×10^{-5} M) to $Fe(bpy)_3(PF_6)_3$ (1.0×10^{-4} M) in MeCN at 298 K with a prolonged reaction time (0−6000 s, 300 s interval). Inset shows time dependence of absorbance at 520 nm.

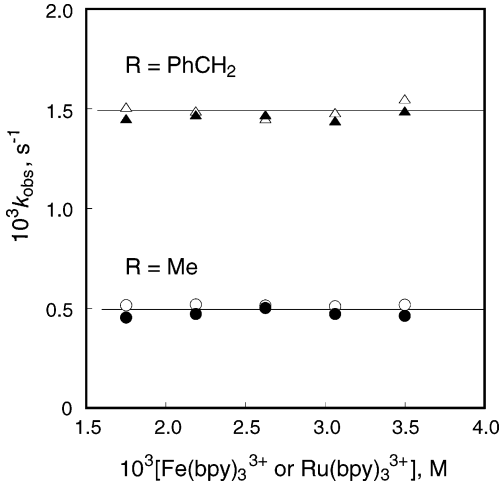

Figure 5. Plots of k_{obs} vs $[Fe(bpy)_3^{3+}]$ or $[Ru(bpy)_3^{3+}]$ in the second electron-transfer oxidation of $(DH)_2Co(R)(py)$ (R = Me and $PhCH_2$) (1.7×10^{-5} M) with $[Fe(bpy)_3^{3+}]$ (○ and △) or $[Ru(bpy)_3^{3+}]$ (● and ▲) in deaerated MeCN at 298 K.

$$[(DH)_2Co^{III}(Me)(py)] + 2[Fe(bpy)_3]^{3+} \rightarrow [(DH)_2Co^{III}] + 2[Fe(bpy)_3]^{2+} + N\text{-MePy}^+ \quad (7)$$

The rate of the second one-electron oxidation step of $(DH)_2Co(PhCH_2)(py)$ obeys first-order kinetics, and the first-order rate constant (k_{obs}) remains the same with variation of the $[Fe(bpy)_3]^{3+}$ concentration used in excess as shown in Figure 5. First-order kinetics have also been reported for the oxidative decomposition of $(DH)_2Co(R)(H_2O)$ at room temperature.[22] The k_{obs} value was determined to be 1.5×10^{-3} s^{-1} at 298 K, and the same value was obtained for the oxidation of $(DH)_2Co(PhCH_2)(py)$ with a stronger oxidant, $[Ru(bpy)_3]^{3+}$ (E°_{red} vs SCE

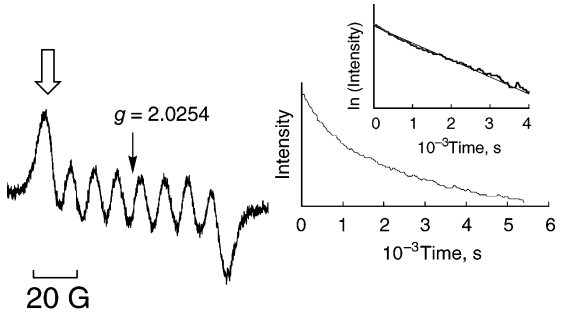

Figure 6. ESR spectrum of $[(DH)_2Co^{IV}(Me)(py)]^+$ produced in the reaction of $(DH)_2Co(Me)(py)$ (1.0×10^{-3} M) with $Ru(bpy)_3(PF_6)_3$ (1.0×10^{-3} M) in deaerated MeCN at 298 K. Decay of the ESR signal of $[(DH)_2Co^{IV}(Me)(py)]^+$ and the first-order plot.

$= 1.24$ V).[23] This constant dependence of k_{obs} on the oxidant concentration indicates that the rate-determining step for the second one-electron oxidation is the cleavage of the Co−C bond of $[(DH)_2Co(R)(py)]^+$ to give R^+ which is readily trapped by the coordinated pyridine to yield the alkylpyridinium ion (Rpy^+).[50] Electron transfer from $(DH_2)Co^{II}(py)$ to $[Fe(bpy)_3]^{3+}$ should proceed efficiently since $(DH_2)Co^{II}(py)$ can act as strong reductant and can also be oxidized by $[Fe(bpy)_3]^{3+}$ in MeCN. In the absence of excess $[Fe(bpy)_3]^{3+}$, the formation of $(DH)_2Co^{II}(py)$ was confirmed by the ESR measurement.[51] Thus, homolytic bond cleavage of the Co(IV)−C bond may be unlikely to occur in this case, because homolytic cleavage would result in the formation of $(DH)_2Co^{III}(py)$. The quantitative formation of alkylpyridinium ion was confirmed by the ^1H NMR spectrum (see Experimental Section).

When the rate-determining step is the Co−C bond cleavage of $[(DH)_2Co(R)(py)]^+$, the rate of formation of $[Fe(bpy)_3]^{2+}$ at the second step should be the same as the rate of disappearance of $[(DH)_2Co(R)(py)]^+$ (eq 8).

$$d[[Fe(bpy)_3]^{2+}]/dt = k_{obs}\{[2[(DH)_2Co(R)(py)]]_0 - [[Fe(bpy)_3]^{2+}]\} = -d[[(DH)_2Co(R)(py)]^+]/dt = k_{obs}[[(DH)_2Co(R)(py)]^+] \quad (8)$$

This was confirmed by monitoring the disappearance of $[(DH)_2Co(R)(py)]^+$ by ESR as shown in Figure 6, where the ESR spectrum of $[(DH)_2Co^{IV}(Me)(py)]^+$ produced in the one-electron oxidation of $(DH)_2Co(Me)(py)$ (1.0×10^{-3} M) with $Ru(bpy)_3(PF_6)_3$ (1.0×10^{-3} M) was measured in deaerated MeCN at 298 K. The slow decay of the ESR signal of $[(DH)_2Co^{IV}(Me)(py)]^+$ obeys first-order kinetics (eq 8, Figure 6 inset), and the observed first-order rate constant ($k_{obs} = 4.9 \times 10^{-4}$ s^{-1}) agrees with the k_{obs} value (5.0×10^{-4} s^{-1}) obtained from the rate of formation of $[Fe(bpy)_3]^{2+}$ at the second step within experimental error (±5%). Thus, what we are observing as the rate of second electron transfer to form $[Fe(bpy)_3]^{2+}$ is the rate of cleavage of the Co^{IV}−C bond of $[(DH)_2Co^{IV}(R)(py)]^+$ produced in the first rapid electron transfer from $(DH)_2Co^{III}(R)(py)$ to $[Fe(bpy)_3]^{3+}$, since the subsequent electron transfer from $(DH_2)Co^{II}(py)$ to $[Fe(bpy)_3]^{3+}$ to produce $[Fe(bpy)_3]^{2+}$ is much faster than the cleavage rate.

In the presence of excess pyridine, the Co(IV)−C bond cleavage of $[(DH)_2Co^{IV}(Me)(py)]^+$ occurs rapidly to yield the *N*-methylpyridinium ion ($Mepy^+$). The rate constants of the Co(IV)−C bond cleavage (k_{obs}) were determined by monitoring the increase of the absorption band due to $[Fe(bpy)_3]^{2+}$ ($\lambda =$ 520 nm) using a stopped-flow technique (see Experimental Section). The k_{obs} value in eq 8 increases with an increasing concentration of pyridine to reach a constant value as shown in Figure 7. This indicates that the rate-determining step for the second electron-transfer step is the cleavage of the Co(IV)−C bond of $[(DH)_2Co^{IV}(Me)(py)]^+$ and that the bond-cleavage step is accelerated by the presence of pyridine as shown in Scheme 1. When pyridine is replaced by a stronger base (3,4-dimethylpyridine), the k_{obs} value becomes larger when compared to the corresponding value of pyridine, whereas a weaker base (3-bromopyridine) gives a smaller k_{obs} value (Figure 7). If the saturated dependence of k_{obs} on base concentrations is caused by the rate-limiting Co(IV)−C bond cleavage followed by the facile reaction with a base, the constant k_{obs} value would be the same regardless of the type of base. Thus, the dependence of the k_{obs} values on the different bases in Figure 8 indicates that $[(DH)_2Co^{IV}(Me)(py)]^+$ forms a complex with a base prior to the heterolytic cleavage of the Co(IV)−C bond (Scheme 1). The fastest rate constant of Co(IV)−C bond cleavage is determined as 83 s^{-1} at 238 K, which is close to that of enzymatic Co−C cleavage of coenzyme B_{12} (20−600 s^{-1}).[9a,10,52]

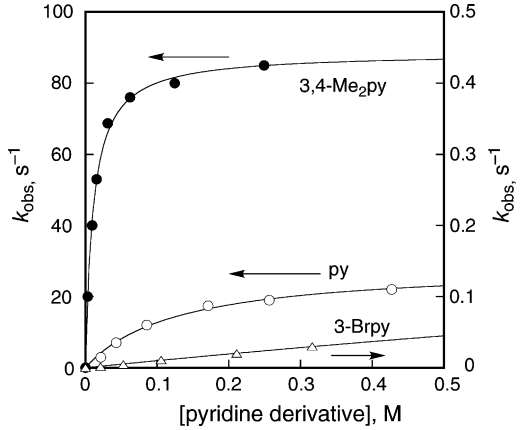

Figure 7. Plots of k_{obs} vs concentrations of pyridine derivatives for the Co(IV)−C bond cleavage of $[(DH)_2Co^{IV}(Me)(py)]^+$ in the presence of pyridine derivatives in deaerated MeCN at −35 °C.

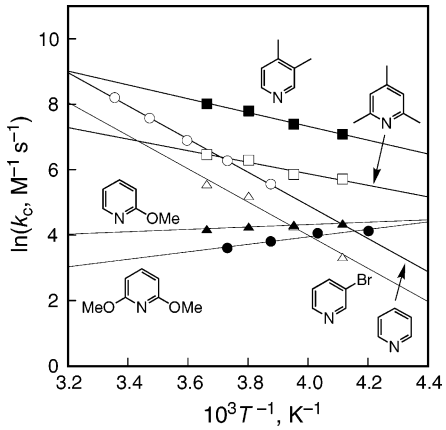

Figure 8. Arrhenius plots of the second-order rate constants (k_c) of the Co(IV)−C bond cleavage of $[(DH)_2Co^{IV}(Me)(py)]^+$ with various pyridine derivatives.

The rates of Co(IV)−C bond cleavage with various bases were determined under experimental conditions so that the k_{obs} values are proportional to the concentrations of the bases at various temperatures. The Arrehenius plots of the second-order rate constants of Co(IV)−C bond cleavage with various bases are shown in Figure 8. The activation enthalpy ($\Delta H^{\ddagger}_{obs}$) value decreases with the decreasing I_p values of bases (Table 4).[37] In the case of 2-methoxypyridine and 2,6-dimethoxypyridine, the

SCHEME 1

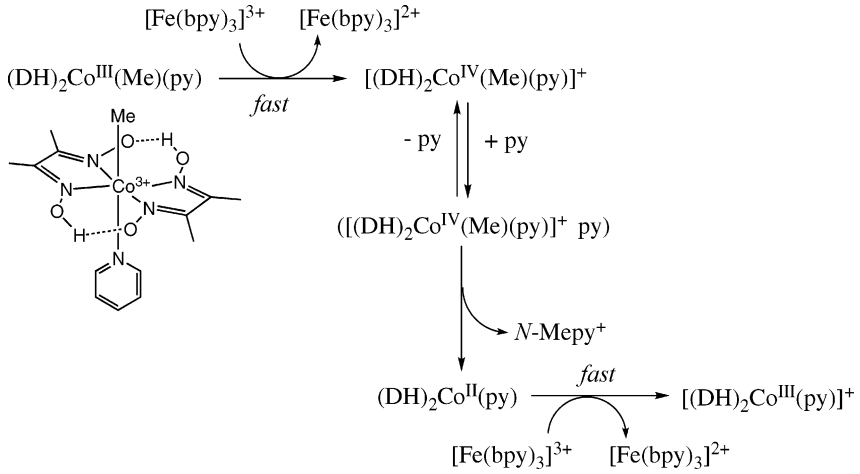

SCHEME 2

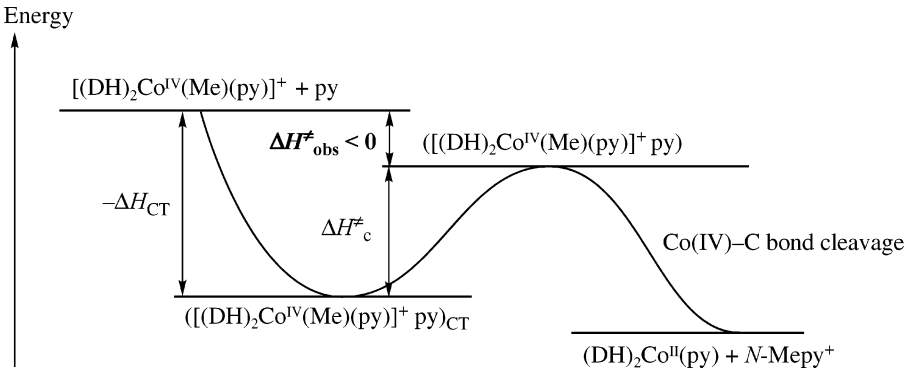

TABLE 4: Ionization Potentials (I_p) of Various Pyridine Derivatives and Activation Parameters for Co(IV)−C Bond Cleavage of $[(DH)_2Co^{IV}(Me)(py)]^+$ in the Presence of Pyridine Derivatives

pyridine	I_p (eV)[a]	$\Delta H^{\ddagger}_{obs}$ (kJ mol^{-1})	$\Delta S^{\ddagger}_{obs}$ (J mol^{-1} K^{-1})
3-Brpy	9.21	42	−8
py	9.15	42	−1
4-Mepy	8.99	26	−23
3,4-Me_2py	8.82	18	−80
2,4,6-Me_3py	8.54	15	−100
2-MeOpy	8.48	−3.0	−190
2,6-$(MeO)_2$py	7.84	−9.5	−220

[a] Calculated by the DFT method (B3LYP/6-31G** basis set).[37]

$\Delta H^{\ddagger}_{obs}$ values are found to be negative (−3.0 and −9.5 kJ mol^{-1}, respectively).

Charge-Transfer Complex between $[(DH)_2Co^{IV}(Me)(py)]^+$ and Pyridine Derivatives. Since $[(DH)_2Co^{IV}(Me)(py)]^+$ is coordinatively saturated, the complex formation between an electron-donating base and $[(DH)_2Co^{IV}(Me)(py)]^+$ which is a strong electron acceptor may be attributed to a charge-transfer (CT) interaction. Pyridine has been known to form strong CT complexes with various electron acceptors.[53] Upon mixing MeCN solutions of $[(DH)_2Co^{IV}(Me)(py)]^+$ and pyridine, we readily observed a new broad absorption band (λ_{max} = 950 nm) as shown in Figure 9. When pyridine is replaced by a weaker electron donor (3-bromopyridine), the absorption band is blue-shifted (840 nm), whereas the addition of a stronger electron donor (4-methylpyridine) results in the red-shift of the absorption band (955 nm). This indicates that the new absorption band is caused by the formation of the CT complex between $[(DH)_2Co^{IV}(Me)(py)]^+$ and the bases.

If the observed CT complex is a real intermediate for the Co(IV)−C bond cleavage, then the observed activation enthalpy ($\Delta H^{\ddagger}_{obs}$) consists of the heat of formation of the CT complex (ΔH_{CT}) and the activation enthalpy of the Co(IV)−C bond cleavage ($\Delta H^{\ddagger}_{c}$). Therefore $\Delta H^{\ddagger}_{obs} = \Delta H_{CT} + \Delta H^{\ddagger}_{c}$ as shown in Scheme 2.[25−27] The ΔH_{CT} value of $[(DH)_2Co^{IV}(Me)(py)]^+$ and pyridine was determined as −29 kJ mol^{-1} from the temperature dependence of the CT absorbance (see Supporting Information S5). With increasing donor ability of the bases, the ΔH_{CT} value is expected to become more negative, whereas the $\Delta H^{\ddagger}_{c}$ value becomes less positive. In this case, the $\Delta H^{\ddagger}_{obs}$ value would be negative under the conditions $\Delta H^{\ddagger}_{c} < -\Delta H_{CT}$.

In conclusion, these results have shown that the observed activation energy for the Co−C bond cleavage of a coenzyme B_{12} model complex can be remarkably decreased by one-electron oxidation. It can also be decreased by the formation of a charge-

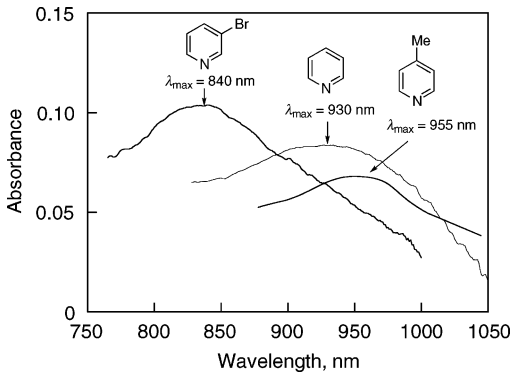

Figure 9. Visible-NIR spectra of CT complexes of $[(DH)_2Co^{IV}(Me)(py)]^+$ (1.5×10^{-2} M) with pyridine derivatives (1.0 M) in MeCN at 298 K.

transfer complex of the resulting alkylcobalt(IV) complex with a base, which leads to the observation of a negative activation energy for the Co(IV)−C cleavage with a strong base. Although $(DH)_2Co^{III}(R)(L)$ is known to act as a nucleophile which can transfer R^- to an electrophile,[54] $[(DH)_2Co^{IV}(R)(L)]^+$, produced by the one-electron oxidation of $(DH)_2Co^{III}(R)(L)$, acts as an electrophile which can transfer R^+ to a nucleophile.

Acknowledgment. This work was partially supported by a Grant-in-Aid (16205020) from the Ministry of Education, Culture, Sports, Science and Technology, Japan.

Supporting Information Available: (S1) NMR data of $(DH)_2Co(R)(L)$, (S2) cyclic voltammogram of $(DH)_2Co(Me)(py)$ (1.0×10^{-2} M) in MeCN, (S3) ESR spectra of $[(DH)_2Co^{IV}(Me)(L)]^+$ (L = H_2O and pyridine), (S4) determination of k_{ex} for the electron self-exchange between $(DH)_2Co^{III}(Me)(py)$ and $[(DH)_2Co^{IV}(Me)(py)]^+$, and (S5) determination of ΔH_{CT} for the CT complex between $[(DH)_2Co^{IV}(Me)(py)]^+$ and pyridine. This material is available free of charge via the Internet at http://pubs.acs.org.

References and Notes

(1) (a) Babior, B. M. *Acc. Chem. Res.* **1975**, *8*, 376. (b) Dolphin, D., Ed. *B_{12}*; Wiley: New York, 1982. (c) Schneider, Z.; Stroinski, A. *Comprehensive B_{12}*; de Gruyter: Berlin, 1987. (d) Toscano, P. J.; Marzilli, L. G. *Prog. Inorg. Chem*. **1984**, *31*, 105. (e) Finke, R. G.; Schiraldi, D. A.; Mayer, B. J. *Coord. Chem. Rev.* **1984**, *54*, 1. (f) Randaccio, L.; Pahor, N. B.; Zangrando, E.; Marzilli, L. G. *Chem. Soc. Rev.* **1989**, *18*, 225. (g) Marzilli, L. G. In *Bioinorganic Catalysis*; Reedijk, J., Ed.; Marcel Dekker: New York, 1993; pp 227−259.

(2) For model studies of molecular rearrangement via radical intermediates see: (a) Newcomb, M.; Miranda, N. *J. Am. Chem. Soc*. **2003**, *125*, 4080. (b) Miranda, N.; Daublain, P.; Horner, J. H.; Newcomb, M. *J. Am. Chem. Soc.* **2003**, *125*, 5260.

(3) (a) Halpern, J. *Science* **1985**, *227*, 869. (b) Halpern, J. *Acc. Chem. Res.* **1982**, *15*, 238.

(4) (a) Tsou, T. T.; Loots, M.; Halpern, J. *J. Am. Chem. Soc*. **1982**, *104*, 623. (b) Ng, F. T. T.; Rempel, G. L.; Halpern, J. *J. Am. Chem. Soc.* **1982**, *104*, 621. (c) Ng, F. T. T.; Rempel, G. L.; Halpern, J. *Inorg. Chim. Acta* **1983**, *77*, L65. (d) Halpern, J.; Kim, S. H.; Leung, T. W. *J. Am. Chem. Soc*. **1984**, *106*, 8317. (e) Geno, M. K.; Halpern, J. *J. Chem. Soc., Chem. Commun.* **1987**, 1052. (f) Ng, F. T. T.; Rempel, G. L.; Mancuso, C.; Halpern, J. *Organometallics* **1990**, *9*, 2762.

(5) Geno, M. K.; Halpern, J. *J. Am. Chem. Soc*. **1987**, *109*, 1238.

(6) Collman, J. P.; McElwee-White, L.; Brothers, P. J.; Rose, E. *J. Am. Chem. Soc*. **1986**, *108*, 1332.

(7) (a) Finke, R. G.; Hay, B. P. *Inorg. Chem.* **1984**, *23*, 3041. (b) Finke, R. G.; Hay, B. P. *Inorg. Chem.* **1985**, *24*, 1278. (c) Hay, B. P.; Finke, R. G. *J. Am. Chem. Soc*. **1986**, *108*, 4820. (d) Hay, B. P.; Finke, R. G. *J. Am. Chem. Soc*. **1987**, *109*, 8012. (e) Koenig, T. W.; Hay, B. P.; Finke, R. G. *Polyhedron* **1988**, *7*, 1499.

(8) Waddington, M. D.; Finke, R. G. *J. Am. Chem. Soc.* **1993**, *115*, 4629.

(9) (a) Hollaway, M. R.; White, H. A.; Joblin, K. N.; Johnson, A. W.; Lappert, M. F.; Wallis, O. C. *Eur. J. Biochem.* **1978**, *82*, 143. (b) Toscano, P. J.; Seligson, A. L.; Curran, M. T.; Skrobutt, A. T.; Sonnenberger, D. C. *Inorg. Chem.* **1989**, *28*, 166.

(10) (a) Licht, S. S.; Gerfen, G. J.; Stubbe, J. *Science* **1996**, *271*, 477. (b) Padmakumar, R.; Padmakumar, R.; Banerjee, R. *Biochemistry* **1997**, *36*, 3713.

(11) (a) Kräutler, B.; Keller, W.; Kratky, C. *J. Am. Chem. Soc.* **1989**, *111*, 8936. (b) Kräutler, B.; Konrat, R.; Stupperich, E.; Färber, G.; Gruber, K.; Kratky, C. *Inorg. Chem.* **1994**, *33*, 4128. (c) Garr, C. D.; Finke, R. G. *Inorg. Chem.* **1993**, *32*, 4414.

(12) Pratt, J. M. *Chem. Soc. Rev.* **1985**, *14*, 161.

(13) (a) Banerjee, R. *Chem. Rev.* **2003**, *103*, 2083. (b) Banerjee, R.; Ragsdale, S. W. *Annu. Rev. Biochem.* **2003**, *72*, 209. (c) Banerjee, R. *Chem. Biol.* **1997**, *4*, 175.

(14) (a) Hill, H. A. O.; Pratt, J. M.; Wiliams, R. J. P. *Chem. Br.* **1969**, *5*, 156. (b) Grate, J. H.; Schrauzer, G. N. *J. Am. Chem. Soc.* **1979**, *101*, 4601.

(15) (a) Nie, S.; Marzilli, L. G.; Yu, N. T. *J. Am. Chem. Soc.* **1989**, *111*, 9256. (b) Nie, S.; Marzilli, P. A.; Marzilli, L. G.; Yu, N. T. *J. Am. Chem. Soc.* **1990**, *112*, 6084.

(16) (a) Garr, C. D.; Sirovatka, J. M.; Finke, R. G. *Inorg. Chem.* **1996**, *35*, 5912. (b) Garr, C. D.; Sirovatka, J. M.; Finke, R. G. *J. Am. Chem. Soc.* **1996**, *118*, 11142. (c) Sirovatka, J. M.; Finke, R. G. *J. Am. Chem. Soc.* **1997**, *119*, 3057. (d) Dong, S.; Padmakumar, R.; Banerjee, R.; Spiro, T. G. *J. Am. Chem. Soc*. **1999**, *121*, 7063. (e) Sirovatka, J. M.; Finke, R. G. *Inorg. Chem.* **1999**, *38*, 1697. (f) Doll, K. M.; Bender, B. R.; Finke, R. G. *J. Am. Chem. Soc*. **2003**, *125*, 10877. (g) Doll, K. M.; Finke, R. G. *Inorg. Chem.* **2003**, *42*, 4849. (h) Doll, K. M.; Finke, R. G. *Inorg. Chem.* **2004**, *43*, 2611.

(17) Mancia, F.; Keep, N. H.; Nakagawa, A.; Leadlay, P. F.; McSweeney, S.; Rasmussen, B.; Bösecke, P.; Diat, O.; Evans, P. R. *Structure* **1996**, *4*, 339.

(18) Jensen, M. P.; Halpern, J. *J. Am. Chem. Soc.* **1999**, *121*, 2181.

(19) (a) Martin, B. D.; Finke, R. G. *J. Am. Chem. Soc*. **1990**, *112*, 2419. (b) Martin, B. D.; Finke, R. G. *J. Am. Chem. Soc.* **1992**, *114*, 585. (c) Finke, R. G.; Martin, B. D. *J. Inorg. Biochem.* **1990**, *40*, 19.

(20) (a) Lexa, D.; Savéant, J. M. *J. Am. Chem. Soc.* **1978**, *100*, 3220. (b) Lexa, D.; Savéant, J. M. *Acc. Chem. Res.* **1983**, *16*, 235.

(21) Halpern, J.; Chan, M. S.; Hanson, J.; Roche, T. S.; Topich, J. A. *J. Am. Chem. Soc.* **1975**, *97*, 1606.

(22) Vol'pin, M. E.; Levitin, I. Y.; Sigan, A. L.; Halpern, J.; Tom, G. M. *Inorg. Chim. Acta* **1980**, *41*, 271.

(23) Fukuzumi, S.; Miyamoto, K.; Suenobu, T.; Van Caemelbecke, E.; Kadish, K. M. *J. Am. Chem. Soc.* **1998**, *120*, 2880.

(24) (a) Ishikawa, K.; Fukuzumi, S.; Goto, T.; Tanaka, T. *J. Am. Chem. Soc.* **1990**, *112*, 1577. (b) Fukuzumi, S.; Ishikawa, K.; Tanaka, T. *Organometallics* **1987**, *6*, 358. (c) Ishikawa, K.; Fukuzumi, S.; Tanaka, T. *Bull. Chem. Soc. Jpn.* **1987**, *60*, 563. (d) Fukuzumi, S.; Kitano, T.; Ishikawa, M.; Matsuda, Y. *Chem. Phys.* **1993**, *176*, 337.

(25) Kiselev, V. D.; Miller, J. G. *J. Am. Chem. Soc.* **1975**, *97*, 4036.

(26) (a) Zaman, K. M.; Yamamoto, S.; Nishimura, N.; Maruta, J.; Fukuzumi, S. *J. Am. Chem. Soc.* **1994**, *116*, 12099. (b) Fukuzumi, S.; Ohkubo, K.; Tokuda, Y.; Suenobu, T. *J. Am. Chem. Soc.* **2000**, *122*, 4286.

(27) (a) Fukuzumi, S.; Endo, Y.; Imahori, H. *J. Am. Chem. Soc.* **2002**, *124*, 10974. (b) Yoder, J. C.; Roth, J. P.; Gussenhoven, E. M.; Larsen, A. S.; Mayer, J. M. *J. Am. Chem. Soc.* **2003**, *125*, 2629.

(28) Schrauzer, G. N. *Inorg. Synth.* **1968**, *11*, 61.

(29) Ishikawa, K.; Fukuzumi, S.; Tanaka, T. *Inorg. Chem.* **1989**, *28*, 1661.

(30) Tada, M.; Nakamura, T.; Matsumoto, M. *J. Am. Chem. Soc*. **1988**, *110*, 4647.

(31) Ishikawa, K.; Fukuzumi, S.; Goto, T.; Tanaka, T. *J. Chem. Soc., Dalton Trans.* **1990**, 85.

(32) (a) Wong, C. L.; Kochi, J. K. *J. Am. Chem. Soc*. **1979**, *101*, 5593. (b) Fukuzumi, S.; Wong, C. L.; Kochi, J. K. *J. Am. Chem. Soc*. **1980**, *102*, 2928.

(33) DeSimone, R. E.; Drago, R. S. *J. Am. Chem. Soc.* **1970**, *92*, 2343.

(34) Perrin, D. D.; Armarego, W. L. F.; Perrin, D. R. *Purification of Laboratory Chemicals*, 4th ed.; Pergamon Press: Elmsford, NY, 1996.

(35) Ford-Smith, M. H.; Sutin, N. *J. Am. Chem. Soc.* **1961**, *83*, 1830.

(36) Mann, C. K.; Barnes, K. K. *Electrochemical Reactions in Nonaqueous Systems*; Marcel Dekker: New York, 1990.

(37) Barrio, L.; Catalán, J.; de Paz, J. L. G. *Int. J. Quantum Chem*. **2003**, *91*, 432.

(38) Shoefield, K. S. *Hetero-Aromatic Nitrogen Compounds*; Plenum Press: New York, 1967; p 146.

(39) Halpern, J.; Topich, J.; Zamaraev, K. I. *Inorg. Chim. Acta* **1976**, *20*, L21.

(40) Topich, J.; Halpern, J. *Inorg. Chem.* **1979**, *18*, 1339.

(41) For stable Co(IV) complexes see: (a) Anson, F. C.; Collins, T. J.; Coots, R. J.; Gipson, S. L.; Richmond, T. G. *J. Am. Chem. Soc*. **1984**, *106*, 5037. (b) Collins, T. J.; Powell, R. D.; Slebodnick, C.; Uffelman, E. S. *J. Am. Chem. Soc.* **1991**, *113*, 8419. (c) Will, S.; Lex, J.; Vogel, E.; Adamian, V. A.; Van Caemelbecke, E.; Kadish, K. M. *Inorg. Chem*. **1996**, *35*, 5577.

(42) The isotropic g and a values correspond to $(g_{||} + 2g_{\perp})/3$ and $(A_{||} + 2A_{\perp})/3$, respectively. The $g_{\perp}$ values are virtually the same as the $g_{||}$ values, whereas the $A_{||}$ values are much larger than the $2A_{\perp}$ values as reported by Halpern et al.[39]

(43) Cheng, K. S.; Horita, N. In *Investigation of Rates and Mechanisms of Reactions*; Hammes, G. G., Ed.; Wiley-Interscience: New York, 1974; Vol. IV, p 565.

(44) Kavarnos, G. J. *Fundamentals of Photoinduced Electron Transfer*; Wiley-VCH: New York, 1993.

(45) (a) Wang, K.; Jordan, R. B. *Can. J. Chem*. **1996**, *74*, 658. (b) Doine, H.; Swaddle, T. W. *Inorg. Chem*. **1991**, *30*, 1858. (c) Setzer, W. N.; Ogle, C. A.; Wildon, G. S.; Glass, R. S. *Inorg. Chem*. **1983**, *22*, 266. (d) Dubs, R. V.; Gahan, L. R.; Sargeson., A. M. *Inorg. Chem*. **1983**, *22*, 2523.

(46) Eberson, L. *Electron-Transfer Reactions in Organic Chemistry*; Springer-Verlag: Berlin, 1987.

(47) Kavarnos, G. J.; Turro, N. J. *Chem. Rev.* **1986**, *86*, 401.
(48) Mikami, K.; Matsumoto, S.; Okubo, Y.; Fujitsuka, M.; Ito, O.; Suenobu, T.; Fukuzumi, S. *J. Am. Chem. Soc.* **2000**, *122*, 2236.
(49) (a) Marcus, R. A.; Eyring, H. *Annu. Rev. Phys. Chem.* **1964**, *15*, 155. (b) Marcus, R. A. *Angew. Chem., Int. Ed. Engl.* **1993**, *32*, 1111.
(50) Vol'pin, M. E.; Levitin, I. Y.; Sigan, A. L.; Nikitaev, A. T. *J. Organomet. Chem.* **1985**, *279*, 263.
(51) A broad ESR signal with $g = 2.013$ due to $(DH)_2Co^{II}(py)$ was observed at 144 K after the reaction of $(DH)_2Co(Et)(py)$ (1.5×10^{-3} M) with 1 equiv of $Fe(bpy)_3^{3+}$ (1.5×10^{-3} M) in MeCN at 298 K for 1 h. For the ESR spectra of low-spin cobalt(II) complexes see: Nishida, Y.; Shimohori, H. *Bull. Chem. Soc. Jpn.* **1973**, *46*, 2406.
(52) (a) Valinski, J. E.; Abeles, R. H.; Fee, J. A. *J. Am. Chem. Soc.* **1974**, *96*, 4709. (b) Hollaway, M. R.; White, H. A.; Joblin, K. N.; Johnson, A. W.; Lappert, M. F.; Wallis, O. C. *Eur. J. Biochem.* **1978**, *82*, 143.
(53) Mulliken, R. S.; Person, W. B. *Molecular Complexes, a Lecture and Reprint Volume*; Wiley-Interscience: New York, 1969.
(54) Fukuzumi, S.; Kitano, T. *Inorg. Chem.* **1990**, *29*, 2558.